Arteriosclerosis, Thrombosis, and Vascular Biology

ORIGINAL RESEARCH

Targeted Inhibition of Gut Microbial TMAO Production Reduces Renal Tubulointerstitial Fibrosis and Functional Impairment in a Murine Model of Chronic Kidney Disease

Nilaksh Gupta, Jennifer A. Buffa, Adam B. Roberts, Naseer Sangwan, Sarah M. Skye, Lin Li, Karen J. Ho, John Varga, Joseph A. DiDonato, W.H. Wilson Tang, Stanley L. Hazen

OBJECTIVE: Gut microbial metabolism of dietary choline, a nutrient abundant in a Western diet, produces trimethylamine (TMA) and the atherothrombosis- and fibrosis-promoting metabolite TMA-N-oxide (TMAO). Recent clinical and animal studies reveal that elevated TMAO levels are associated with heightened risks for both cardiovascular disease and incident chronic kidney disease development. Despite this, studies focusing on therapeutically targeting gut microbiota-dependent TMAO production and its impact on preserving renal function are limited.

APPROACH AND RESULTS: Herein we examined the impact of pharmacological inhibition of choline diet-induced gut microbiota-dependent production of TMA, and consequently TMAO, on renal tubulointerstitial fibrosis and functional impairment in a model of chronic kidney disease. Initial studies with a gut microbial choline TMA-lyase mechanism-based inhibitor, iodomethylcholine, confirmed both marked suppression of TMA generation, and consequently TMAO levels, and selective targeting of the gut microbial compartment (ie, both accumulation of the drug in intestinal microbes and limited systemic exposure in the host). Dietary supplementation of either choline or TMAO significantly augmented multiple indices of renal functional impairment and fibrosis associated with chronic subcutaneous infusion of isoproterenol. However, the presence of the gut microbiota-targeting inhibitor iodomethylcholine blocked choline diet-induced elevation in TMAO, and both significantly improved decline in renal function, and significantly attenuated multiple indices of tubulointerstitial fibrosis. Iodomethylcholine treatment also reversed many choline diet-induced changes in cecal microbial community composition associated with TMAO and renal functional impairment.

CONCLUSIONS: Selective targeting of gut microbiota-dependent TMAO generation may prevent adverse renal structural and functional alterations in subjects at risk for chronic kidney disease.

Key Words: cardiovascular disease ∎ fibrosis ∎ isoproterenol ∎ microbiota ∎ trimethylamine

It is becoming increasingly apparent that gut microbiota play a role in both the development of chronic kidney disease (CKD) and its progression to end-stage renal disease (ESRD).[1–5] The gut microbiome contributes to the generation of metabolites that display uremic toxicity[6–8] and that can potentially contribute directly to the pathophysiology of both CKD and ESRD. For example, gut microbiota-derived uremic toxins have been implicated in CKD progression through promotion of adverse pathophysiologic changes in the kidney, including fibrosis,[9] loss of renal tubular function,[10,11] and reduction in glomerular filtration rate (GFR).[12] Despite this growing appreciation, understanding of the direct gut microbiota participants involved is limited, since neither the

Nonstandard Abbreviations and Acronyms

CKD	chronic kidney disease
Coll 1a1	collagen type I-α1
ESRD	end-stage renal disease
FMO	flavin monooxygenase
GFR	glomerular filtration rate
IMC	iodomethylcholine
TGF-β	transforming growth factor-β
TIMP1	tissue inhibitor of metalloproteinase 1
TMA	trimethylamine
TMAO	trimethylamine N-oxide
α-SMA	α-smooth muscle actin

Highlights

- The suicide substrate inhibitor iodomethylcholine, which is nonlethal to gut microbes, selectively targets gut microbial trimethylamine-lyase activity and suppresses choline diet induced trimethylamine, trimethylamine N-oxide, renal functional impairment (glomerular filtration rate and Cystatin C) and injury (albumin to creatinine ratio).
- The gut microbial choline trimethylamine-lyase inhibitor, iodomethylcholine, suppresses choline-diet-induced renal tubulointerstitial fibrosis, and profibrotic gene expression.
- The present studies reveal a novel approach that targets the gut microbial trimethylamine N-oxide pathway and both prevents renal functional decline and tubulointerstitial fibrosis in vivo, while simultaneously limiting systemic exposure and potential for adverse side effects in the host.

microbes, nor the specific microbial enzymes and their nephrotoxic products are unambiguously defined. Consequently, therapeutic strategies that limit gut microbiota-dependent contributions to the clinical progression of CKD are limited. Rather, many recent studies in this area have focused on preventing the accumulation of gut microbiome-derived uremic toxins in subjects for whom extensive renal functional decline has already occurred (ie, ESRD) by adjusting the length and types of dialysis in an effort to improve potential toxic metabolite elimination.[13,14] Other recent studies have pursued the use of probiotics to alter microbial composition[15,16] or the use of resins[17] to intercept gut microbial metabolites that are made before systemic adsorption. Unfortunately, most of these treatments display inherent disadvantages, including adverse side effects, high cost, and, notably, they often have sought to reduce levels after the renal functional decline and fibrosis have occurred (eg, in ESRD). Consequently, the targeting of a gut microbiota pathogenic process for the prevention or treatment of CKD has yet to become adopted into clinical practice.

The meta-organismal production of trimethylamine N-oxide (TMAO) has recently emerged as a gut microbiota-dependent metabolite with both clinical and mechanistic links to cardiovascular and metabolic diseases, including CKD. TMAO production begins with nutrient precursors abundant in red meat and a Western diet, such as phospatidylcholine, choline, and carnitine. Gut microbes can use these nutrient precursors as a carbon fuel source, generating as a waste product trimethylamine (TMA), which, following absorption into the portal blood, is converted with near first-pass kinetics within the liver to TMAO by a family of hepatic FMOs (flavin monooxygenases), particularly FMO_3. Clinical studies have demonstrated that systemic circulating TMAO levels are associated with adverse CVD events (eg, heart attack, stroke, and death) within multiple cardiovascular and CKD cohorts.[1,18,19] Moreover, numerous animal model studies indicate that microbiota-dependent

TMAO generation can directly contribute to the pathogenesis of both atherosclerosis and thrombosis. In these animal studies, a diet supplemented with choline to levels consistent with that observed in omnivorous subjects on a Western diet results in elevation in TMAO to levels observed in humans, and after chronic exposure, was shown to foster both progressive renal functional impairment and enhanced fibrosis.[1] Human subject intervention studies have similarly shown that provision of oral supplementary choline to healthy volunteers substantially increases TMAO levels, with concurrent increases in platelet reactivity to submaximal levels of agonists.[20] In addition, community-based clinical studies, such as the Framingham Heart Study (in subjects with normal renal function at baseline), have reported a strong association between high circulating TMAO and choline levels at baseline and incident risk for future development of CKD.[21]

Given the potential contribution of gut microbiota-dependent generation of TMAO to both cardiovascular and metabolic diseases, substantial effort has recently been focused on developing approaches to selectively target the meta-organismal TMAO pathway. Toward that end, we have recently developed and characterized use of poorly adsorbed, nonlethal small molecule inhibitors of gut microbiota-dependent conversion of choline→TMA (ie, choline TMA-lyase activity inhibition) as an effective means of attenuating atherosclerosis[22] and thrombosis.[23] To date, little is known about the potential for therapeutically targeting the TMAO pathway to prevent renal functional impairment and fibrosis in animal models of CKD.

We have recently developed a family of mechanism-based suicide substrate inhibitors designed to be minimally absorbed into the host, but rather, to selectively accumulate within and target gut microbe production

of TMA in a nonlethal fashion. Moreover, the new family of inhibitors (halomethylcholines) were shown to be over 10 000-fold more potent (sub-nanomolar IC50) than prior reported microbial choline TMA-lyase inhibitors and to both suppress microbial production of TMA and plasma TMAO levels in the host.[23] Using several members of this family of mechanism-based inhibitors and animal models of thrombosis (carotid artery injury), we showed inhibition of diet-dependent enhancement in both platelet responsiveness and in vivo thrombosis potential, without enhancing bleeding risks.[23] Use of these gut microbe−targeting inhibitors for suppression of renal functional decline and fibrosis in a model of CKD has yet to be reported. Herein we evaluate the impact of iodomethylcholine (IMC), a prototypic mechanism-based gut microbial choline TMA-lyase inhibitor, on choline diet-induced adverse renal structural and functional changes in a chronic sympathetic-driven (isoproterenol infusion) model of CKD.

MATERIALS AND METHODS

The authors declare that all supporting data are available within the article and its in the Data Supplement.

Experiment Design

To avoid the potential nephroprotective effects of estrogen,[24–27] only male C57BL/6J mice were used (The Jackson Laboratory, Bar Harbor, ME). Mice were kept on a 12:12 hour light-dark cycle with free access to diet and water. Mice were bred and maintained on Tekled (Envigo) diet 2918 (an irradiated global 18% protein rodent diet). Upon enrollment in studies, mice were initially placed on the indicated diets/groups: (1) Control diet: Teklad (Envigo) 2018 (a global 18% protein rodent diet), a standard normal rodent diet without added choline that in mass spectrometry studies we confirmed contains 0.08 g% total choline content; (2) TMAO diet: the Control diet supplemented with an additional 0.3 g% TMAO; (3) Choline diet: the Control diet supplemented with an additional 1 g% choline (ie, 1.08 g% total choline); and (4) Choline+IMC diet: the Control diet supplemented with an additional 1 g% choline+0.06 g% IMC. After 1 week of diet alone, isoproterenol was subcutaneously infused via mini-osmotic pump (Alzet, Catalog No. 1004, Colorado City, CO) at a concentration of 30 mg/kg per day for 28 days, along with continued administration of the indicated diet/intervention arms. All animal model studies were approved by the Institutional Animal Care and Use Committee at the Cleveland Clinic.

To examine intestinal luminal content, animals were humanely euthanized by anesthesia overdose (>300 mg/kg ketamine+30 mg/kg xylazine), and the small intestine, cecum, and colon were collected. Luminal content was removed, and levels of metabolites were quantified as previously described.[23] LC−MS/MS was used to quantify plasma levels of TMAO, TMA, choline, betaine, IMC, and iodomethylbetaine and urinary levels of creatinine, as previously described.[22,23,28,29] Their isotope (d9)-labeled analogs were used as internal standards. d2-IMC was synthesized and used as an internal standard for IMC

quantification, and d9-betaine was used as an internal standard for iodomethylbetaine quantification, as previously described.[23] LC−MS/MS analyses were performed on a Shimadzu 8050 triple quadrupole mass spectrometer.

Renal Function Assessment

Transdermal FITC-sinistrin clearance was performed to measure GFR in conscious mice, as previously described.[30–32] The FITC-sinistrin half-life was calculated using a 3-compartment model with linear fit using MPD Studio software (MediBeacon, Mannheim, Germany). Cystatin C was measured 4 weeks after isoproterenol exposure using a commercially available mouse ELISA (R&D systems, Minneapolis, MN), as previously described.[1] Urinary albumin was measured with a murine microalbuminuria ELISA kit (Ethos Biosciences, Catalog No. 1011, Philadelphia, PA) in accordance with manufacturer's protocol.

Renal Histology

At time of euthanization, kidneys were collected, fixed in formalin, and embedded in paraffin. For Picrosirius red staining, deparafinized 5 μm serial kidney sections were stained with Picrosirius red staining solution (0.5 g direct red [Sigma-Aldrich] dissolved in 500 mL picric acid [Sigma-Aldrich]). The kidney sections were mounted under a Leica DM 2500 microscope and digitized with a QImaging MicroPublisher 5.0 RTV camera for wide-field microscopy. Quantitative morphometric analysis was performed as previously described.[1] Briefly, collagen volume was determined on cortical fields (at least 10 from each animal) lacking major blood vessels using automated (for batch analysis) and customized algorithms/scripts (ImageIQ Inc, Cleveland, OH) written for Image Pro Plus 7.0. Briefly, a set of representative images was chosen that demonstrated a wide range of staining intensities and prevalence. In an automated script, these training images were loaded one after another prompting the user to delineate red pixels representing positive collagen staining using an interactive color picking tool. An iterative color profile or classifier was generated and subsequently applied to all images in a given directory using a fully automated algorithm. Positive pixels, as defined by the color profile, were segmented and summed to provide positive staining area. Total tissue area was determined by extracting the saturation channel, applying a lo-pass filter, and thresholding the result. Any area within the general tissue boundary that was empty (ie, white) was removed by converting the original image to grayscale and applying a fixed threshold for nonbackground pixels on adequately white-balanced images. Finally, total tissue area and total stained area were exported to Excel. For postprocessing verification, segmented regions were superimposed onto the original image (green outlines) and saved for each image analyzed. For Masson trichrome staining, slides were deparaffinized, rehydrated, and stained using a commercially available kit for Masson trichrome staining (Sigma-Aldrich). Five to 10 nonoverlapping high-powered fields from the cortical area of each mouse kidney were graded for fibrotic changes on a scale of 0 to 3 by 2 investigators blind to the treatment group.

Immunohistochemistry Analysis

Slides were deparaffinized and rehydrated. Antigen retrieval was performed in sodium citrate buffer (pH 6) in a pressurized

decloaking chamber at 110°C for 5 minutes. Slides were incubated with the anti-α-SMA (α-smooth muscle actin) primary antibody (rabbit polyclonal antibody, Abcam No. ab5694) at a 1:500 (0.4 µg/mL) dilution overnight. The biotin-conjugated donkey anti-rabbit secondary antibody (Jackson Immuno No. 711-065-152) was used at a 1:250 dilution for 1 hour. Staining was developed using an avidin-biotin complex conjugated to HRP and DAB substrate with a reaction time of ≈10 minutes. Five nonoverlapping high-powered fields from the cortical area of each kidney were graded for prevalence of staining on a scale of 0 to 2 by 2 investigators blind to the treatment group.

RNA Extraction, Reverse Transcription, and Quantitative Polymerase Chain Reaction

Explanted kidneys were homogenized in RLT buffer complemented with β-mercaptoethanol using TissueLyser II (Qiagen) at 25 m/s for 2 minutes (2 rounds). Total mRNA from kidney was extracted with RNA fibrous mini kit (Qiagen) according to the manufacturer's protocol. DNAse digestion was performed using the RNase-free DNAse Set (Qiagen). Total RNA extractions were analyzed for purity and concentration using the NanoDrop 1000 spectrophotometer (Thermo Fisher). RNA samples were diluted to a final concentration of 100 ng/µL, and cDNA was prepared using high-capacity cDNA reverse transcription kit (Applied Biosystems). Normalization was to GAPDH gene. Real-time polymerase chain reaction with an ABI Prism 7000 sequence detection system (Applied Biosystems), based on TaqMan fluorescence methodology, was used for mRNA quantification. TaqMan probe and primers were purchased as TaqMan gene expression assays-on-demand from Applied Biosystems for GAPDH (Mm99999915_g1), TGF-β (transforming growth factor-β; Mm01227699_m1), Coll 1a1 (collagen type I-α1; Mm00801666_g1), TIMP1 (tissue inhibitor of metalloproteinase 1; Mm01341361_m1), and α-SMA; Mm00725412_s1). Expression level of each tested gene was analyzed in duplicate for each sample and normalized to the expression of the housekeeping reference gene GAPDH. Gene expression was calculated by using the comparative Ct method, using kidney samples of control-treated mice as calibrator samples.

Cecal Microbiota Composition Analyses

16S rRNA gene sequencing methods were adapted from the methods developed for the National Institutes of Health-Human Microbiome Project.[33] Briefly, genomic DNA was extracted from mouse ceca using a MoBio Power Soil DNA extraction kit (Omega, Norcross, GA). The 16S rRNA V4 region was amplified and sequenced. Raw 16S amplicon sequence and metadata were demultiplexed using *split_libraries_fastq.py* script implemented *in QIIME1.9.1.*[34] The demultiplexed fastq file was split into sample-specific fastq files using *split_sequence_file_on_sample_ids.py* script from *Qiime1.9.1.*[34] Individual fastq files without nonbiological nucleotides were processed using Divisive Amplicon Denoising Algorithm pipeline.[35] The output of the dada2 pipeline (feature table of amplicon sequence variants) was processed for alpha and beta diversity analysis using phyloseq,[36] and microbiomeSeq (http://www.github.com/umerijaz/microbiomeSeq) packages in R. Alpha diversity estimates were measured within group

categories using estimate_richness function of the phyloseq package.[36] Nonmultidimensional scaling (NMDS) was performed using Bray-Curtis dissimilarity matrix[37] between groups and visualized by using *ggplot2* package.[38] We assessed the statistical significance ($P<0.05$) throughout and whenever necessary adjusted P values for multiple comparisons according to the Benjamini and Hochberg method to control False Discovery Rate[39] while performing multiple testing on taxa abundance according to sample categories. We performed an ANOVA among sample categories while measuring α-diversity using the *plot_anova_diversity* function in *microbiomeSeq* package (http://www.github.com/umerijaz/microbiomeSeq). Permutational multivariate ANOVA with 999 permutations was performed to test the statistical significance of the nonmultidimensional scaling patterns with the ordination function of the microbiomeSeq package. Linear regression was performed on taxa abundances against TMAO, GFR, cystatin C, and ACR levels in R.[40] 5 872 030 total reads were generated postquality filtering, with an average of 167 772 reads per sample. Samples were rarefied to a depth of 102 000 sequences/sample.

Statistical Analysis

All experimental data are presented as the mean±SEM values of biological replicates. The D'Agostino-Pearson test was used to test for normality. Unless otherwise stated in methods, statistical significance among different treatment groups was calculated using nonparametric 1-way ANOVA followed by Dunn post hoc test. Global P values were calculated using the nonparametric Kruskal-Wallis test. For correlation between plasma TMAO levels and fibrosis indices, P values were calculated using nonparametric Spearman correlation. Statistical tests used to compare conditions are also indicated in figure legends. GraphPad PRISM 8.0 and R 3.4.4 (Vienna, Austria, 2018) were used to generate graphs and statistics. A $P<0.05$ was considered statistically significant.

RESULTS

The Suicide Substrate Inhibitor IMC Selectively Targets Gut Microbial TMA-Lyase Activity in the Isoproterenol Infusion Model

In the present study, we elected to use chronic isoproterenol infusion as a model of CKD, since it previously has been shown to accelerate renal functional decline and tubulinterstitial fibrosis in animal models.[43,47,48] CKD and ESRD are often accompanied by sympathetic hyperreactivity, which has been shown to contribute to both progressive renal functional decline and high rate of cardiovascular events in these patients.[41–43] Further, sympathetic (adrenergic) overdrive has been noted even in early stages of renal disease, and which parallels the severity of renal functional decline despite adequate blood pressure control.[44] It is also of interest that sympatho-inhibitory drugs have been shown to have renoprotective effects in subjects independent of blood pressure control, further implicating sympathetic stimulation as a contributor to CKD development in humans.[45,46] While

the isoproterenol infusion model thus simulates many features of CKD observed in humans, we felt it prudent to first confirm that our proposed gut microbe-targeting drug, IMC, still selectively targeted the gut microbiome compartment in this model since sympathetic hyper-stimulation has also been shown to induce numerous changes in the gastrointestinal tract including altera-tions (enhancement) in gastric motility, hypersecretion of mucus production, and enhanced gut leakiness.[49–53] Sub-cutaneous osmotic mini-pumps containing isoproterenol were, therefore, placed in several groups of mice (Fig-ure 1) for initial pharmacokinetic studies with IMC. Fol-lowing several weeks of exposure, mice were euthanized and both serum and intestinal luminal contents were recovered for mass spectrometry analyses. Notably, IMC accumulated to millimolar (0.7–1.3 mmol/L) levels within the cecum and colon where the majority of gut micro-biota reside (Figure 1A), while completely suppressing choline diet-induced production of microbial TMA, and consequently TMAO (Figure 1B and 1E). While only mini-mally detectable levels of choline were present within the intestinal luminal contents in the choline-fed mice, addi-tion of IMC both blocked TMA production (Figure 1B) and resulted in further gut microbiota accumulation of choline, the immediate precursor to TMA (Figure 1C). Intestinal luminal levels of betaine, a major metabolite of choline, were mostly unaffected (Figure 1D). Interest-ingly, there was TMAO detected in the lumen within the choline-supplemented mice (presumably either by diffu-sion from the host or enterohepatic recycling) but the addition of inhibitor (IMC) completely suppressed luminal presence of TMAO in the choline-fed mice (Figure 1E). Finally, the primary metabolite of IMC, iodomethylbetaine, was also observed within the gut lumen (Figure 1F).

In parallel analyses, we examined plasma levels of IMC and TMAO-related pathway metabolites in all 3 groups of mice. While both TMA ($P=0.01$ versus control, Fig-ure 2A) and TMAO ($P=0.04$ versus control, Figure 2B) were significantly increased in the presence of choline diet, addition of IMC dramatically suppressed the choline diet-induced increases (for TMA $P=0.006$; for TMAO $P=0.001$; Figure 2A and 2B). In contrast to the gut-lumen contents, where it accumulated to millimolar levels, IMC was virtually undetectable in plasma (Figure 2C). In addition, plasma levels of iodomethylbetaine, the primary metabolite of IMC, were only minimally increased in the presence of the drug (Figure 2D). Plasma levels of cho-line (Figure 2E) and betaine (Figure 2F), however, were not affected by choline diet or by IMC. These findings show that within the isoproterenol infusion model, IMC potently suppresses gut microbiota-driven formation of TMA, and consequently TMAO, within the gut microbial compartment, despite alterations in intestinal motility previously described for chronic sympathetic stimula-tion,[49–51] while also showing little evidence of systemic exposure within the host.

IMC Suppresses Choline Diet-Induced TMA, TMAO, Renal Functional Impairment, and Injury

In additional studies, the impact of either choline diet-induced increases in gut microbial TMAO generation or IMC treatment on renal function and adverse renal remodeling were examined in the isoproterenol infusion model (Figures 3 and 4). In another group of isoproterenol treated mice, we also examined the effect of direct provi-sion of dietary TMAO (0.3 g%) on renal function. Analysis of plasma from mice in all treatment groups pre- and post- (4 weeks) isoproterenol infusion revealed that, compared with control, both TMAO ($P<0.0001$) and choline diet ($P<0.0001$) feeding significantly increased plasma TMAO levels throughout the isoproterenol infusion period, while the presence of IMC completely suppressed the choline diet-induced increase in plasma TMAO levels ($P<0.0001$ versus 1% choline, Figure 3B and 3C). In parallel studies, mouse renal function was directly assessed by transcuta-neous measurement of GFR, as described under Mate-rials and Methods. Notably, both TMAO ($P=0.03$ versus control, Figure 4A) and choline diet feeding ($P=0.003$ versus control, Figure 4A) significantly decreased mouse GFR, 31% and 35% respectively, whereas addition of the gut microbial choline TMA-lyase inhibitor IMC virtually completely prevented the choline diet-induced decrease in GFR ($P=0.006$ versus 1% choline and $P=0.83$ versus control; Figure 4A). In additional studies, plasma levels of Cystatin C, an early marker of renal tubular injury, were examined. Plasma Cystatin C levels were increased by 32% (relative to control) in the mice directly fed supple-mental TMAO ($P=0.0006$, Figure 4B), and by 26% (rela-tive to control) in mice placed on the supplemental dietary choline ($P=0.004$, Figure 4B). Notably, addition of IMC markedly attenuated dietary choline-induced increases in plasma Cystatin C ($P=0.02$ versus 1% choline, and $P=0.63$ versus control; Figure 4B). Urinary albumin-to-creatinine ratio (ACR) also was significantly increased with TMAO ($P=0.005$ versus control, Figure 4C) and choline diet feeding ($P=0.001$ versus control, Figure 4C), while provision of IMC completely suppressed the choline diet-induced increase in ACR ($P=0.005$ versus 1% cho-line and $P=0.82$ versus control; Figure 4C). Collectively, these data demonstrate that provision of the gut microbial choline TMA-lyase inhibitor, IMC, both suppressed TMAO levels and completely blocked multiple indices of choline diet-induced renal functional impairment and injury.

The Gut Microbial Choline TMA-Lyase Inhibitor, IMC, Suppresses Choline Diet-Induced Renal Tubulointerstitial Fibrosis

We next quantified the extent of renal tubulointerstitial fibrosis in formalin-fixed samples using two independent approaches. We observed a significant 4-fold increase in picrosirius red staining with conditions associated with
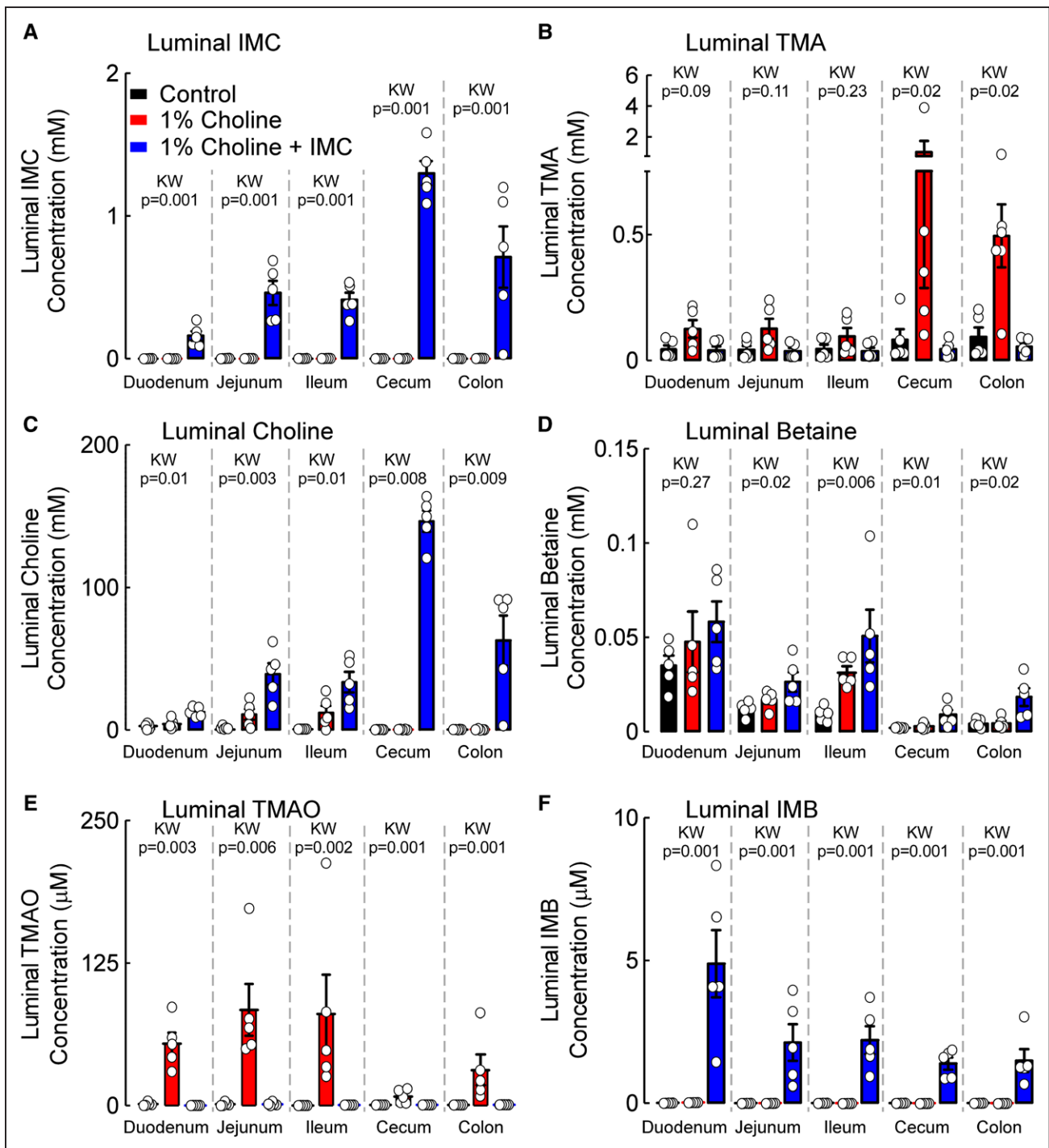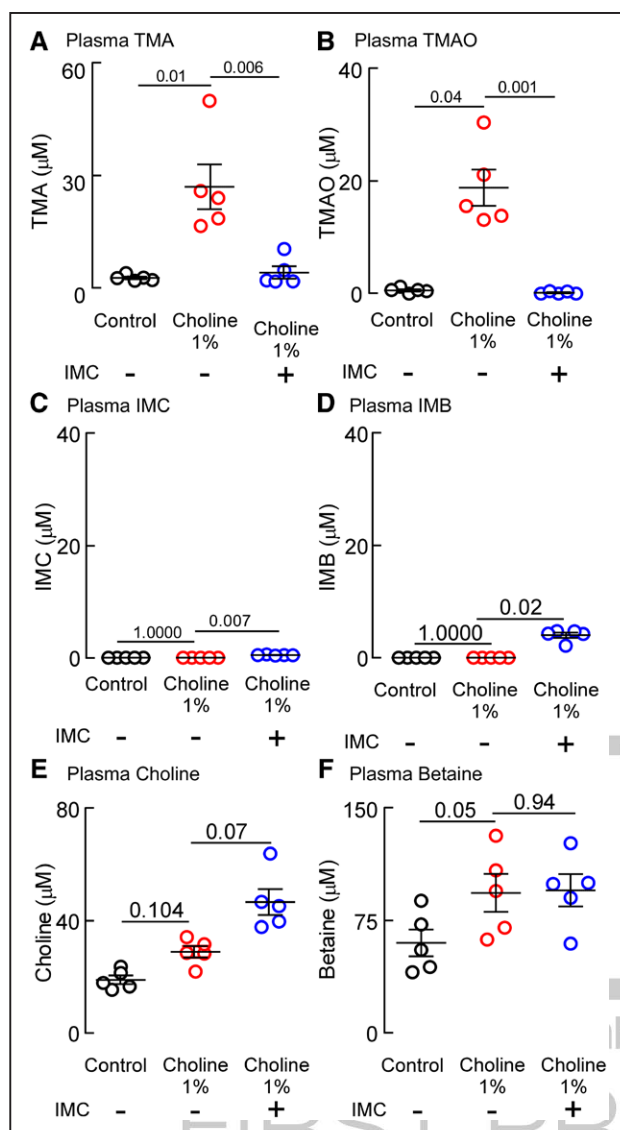
Figure 1. Microbial trimethylamine (TMA)-lyase inhibitor, iodomethylcholine (IMC), selectively accumulates within the gut microbial compartments.
Luminal concentrations of (**A**) IMC, (**B**) TMA, (**C**) choline, (**D**) betaine, (**E**) TMA N-oxide (TMAO), and (**F**) iodomethylbetaine (IMB). Results represent the mean±SEM (n=5), and global P value for each luminal segment was obtained by nonparametric Kruskal-Wallis (KW) test.

higher systemic TMAO (ie, with either TMAO diet feeding [$P<0.0001$ versus control] or choline diet [$P<0.0001$ versus control]; Figure 5A and 5B). In contrast, in the presence of the mechanism-based suicide inhibitor IMC, plasma TMAO levels were suppressed, and a significant reduction in the diet-dependent increase in renal tubulointerstitial fibrosis ($P=0.03$ versus 1% choline, Figure 5A

and 5B) was observed. When renal tubulointerstitial fibrosis and collagen deposition were instead quantified by mason trichrome staining, significant increases were again noted with both TMAO ($P<0.0001$ versus control, Figure 6A and 6B) and choline-supplemented diet groups ($P<0.0001$ versus control, Figure 6A and 6B), and addition of IMC significantly attenuated the choline

Figure 2. Microbial trimethylamine (TMA)-lyase inhibitor iodomethylcholine (IMC) significantly reduces gut-microbe dependent plasma TMA and TMA N-oxide (TMAO) levels.
Plasma concentrations of (**A**) TMA, (**B**) TMAO, (**C**) IMC, (**D**) iodomethylbetaine (IMB), (**E**) choline, and (**F**) betaine. Results represent the mean±SEM (n=5), and the *P* value among different treatments was determined by nonparametric 1-way ANOVA after Dunn post hoc test.
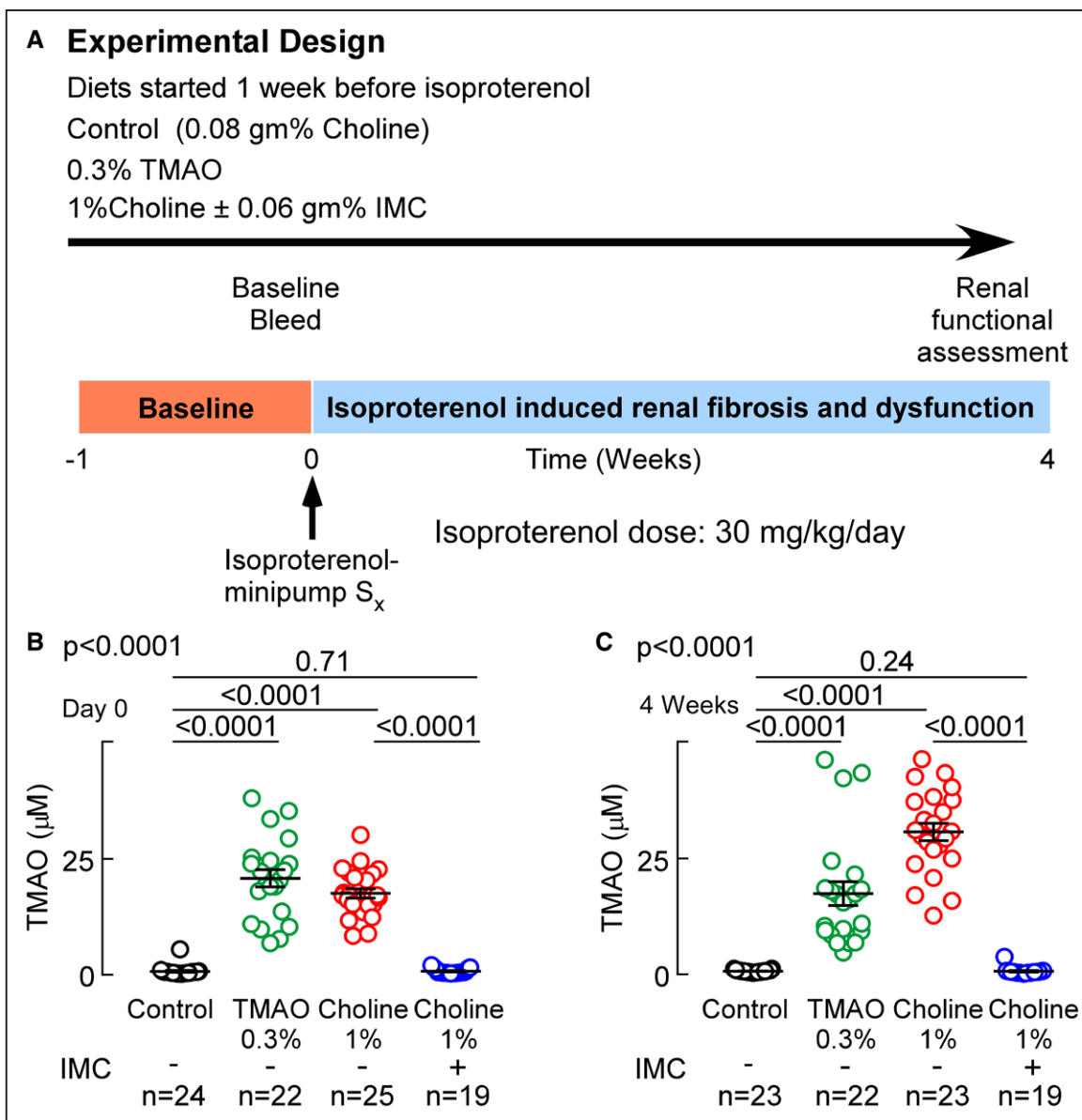
The Gut Microbiota-Targeting Choline TMA-Lyase Inhibitor IMC Prevents Multiple Renal Profibrotic Gene Expression Changes

In mRNA analyses, we observed modest but statistically significantly increases in TGF-β gene expression in renal tissues recovered from mice fed the choline-supplemented diet (*P*=0.01 versus control, Figure 6A). Moreover, addition of IMC significantly suppressed choline diet-induced increases in TGF-β gene expression (*P*<0.0001 versus 1% choline, Figure 7A). Similar patterns of profibrotic gene expression changes were observed (increase with choline diet, reversal of choline diet-induced increase with addition of IMC) with several additional profibrotic genes, including the fibrillar collagen gene *col1a1*, the inhibitor of tissue metalloproteinases *timp1*, and α-SMA, a commonly used myofibroblast marker (*P*<0.0001, *P*=0.008, and *P*=0.001, respectively, Figure 7B through 7D). Direct provision of TMAO, which resulted in intermediate (more modest) TMAO increases (compared with the choline-fed animals), similarly resulted in more modest increases in gene expression levels of the target genes examined, with only some reaching statistical significance (in comparisons with control group; Figure 7).

Gut Microbial Choline TMA-Lyase Inhibition Attenuates Choline Diet-Induced-α-SMA Protein Expression

We also performed quantitative immunohistochemical staining for protein level of murine α-SMA in renal tissues, as described in Materials and Methods. α-SMA protein tissue staining was significantly increased in mice chronically exposed to higher levels of TMAO, whether it be via direct provision of dietary TMAO (*P*<0.0001 versus control, Figure 8A and 8B) or choline-supplemented diet (*P*<0.0001 versus control, Figure 7A and 7B). Importantly, provision of the gut microbiota-targeting inhibitor IMC significantly attenuated the choline diet-induced changes, thereby attenuating the extent of α-SMA tissue staining quantified (*P*=0.007 versus 1% choline, Figure 8A and 8B). We also noted a significant increase in α-SMA protein among TMAO-fed animals, while α-SMA mRNA expression did not change. We speculate that α-SMactin mRNA expression changes were not persistent through to the time of animal euthanization despite the chronic (1 month) exposure to elevated circulating TMAO levels and sympathetic hyper-stimulation, whereas protein (and fibrosis) are more persistent (ie, a difference in lifespan/persistence of RNA versus protein). Consistent with this, rapid and persistent elevations in α-SMA protein independent of RNA transcript abundance have previously been noted.[54–56] Notably, when examined across all groups of mice, a strong dose-dependent relationship was observed between systemic (plasma) TMAO levels

diet-induced renal tubulointerstitial fibrosis (*P*=0.007 versus 1% choline, Figure 6A and 6B). Global analyses across all groups of animals revealed a strong dose-dependent relationship between systemic TMAO levels and extent of renal tubulointerstitial fibrosis, as quantified using either picrosirius red staining (*r*=0.76, *P*<0.0001, Figure 5C) or Masson trichrome staining (*r*=0.73, *P*<0.0001, Figure 6C). These data thus show that gut microbiota-generated TMA(O) provokes renal functional decline and enhanced fibrosis, and that targeted inhibition of microbial choline TMA-lyase activity with an inhibitor that is poorly absorbed by the host, IMC, blocks both the renal functional decline and tubulointerstitial fibrosis observed in this model.

Figure 3. Choline trimethylamine (TMA)-lyase inhibitor, iodomethylcholine (IMC), suppresses gut-microbe dependent plasma TMA N-oxide (TMAO) levels.
A, Wild-type C57BL/6J male mice (10 wk old) were fed indicated diets for 7 days. After 7 days, isoproterenol (30 mg/kg BW per day, 28 days) was infused subcutaneously with vehicle, via osmotic mini-pumps along with the indicated diets for 4 wk. Mice were humanely euthanized at the end of the study, and kidneys were dissected and frozen in liquid nitrogen (for protein or mRNA extraction) and fixed in 4% buffered formaldehyde (for histology and immunohistochemistry). **B**, Plasma TMAO levels at day 0 (before isoproterenol infusion) and (**C**) at 4 wk (after isoproterenol perfusion). Results are presented as mean±SEM. Global *P* value shown was obtained by nonparametric Kruskal-Wallis, and the *P* value among different treatments was determined by nonparametric 1-way ANOVA after Dunn post hoc test.

and quantitation of renal α-SMA protein content (r=0.75, P<0.0001, Figure 8C).

Gut Microbial Choline TMA-Lyase Inhibition Reverses Many Choline Diet-Induced Gut Microbiota Community Changes

In further studies, we examined the impact of dietary choline supplementation and IMC treatment on gut microbial community structure, with a focus on TMAO-associated taxa whose proportions are also linked to measures of renal functional impairment. Cecal microbial DNA encoding 16S ribosomal RNA was sequenced and, in initial analyses, nonmetric multidimensional scaling was performed among the 4 groups of mice. Four distinct, nonoverlapping clusters were observed (Figure 9A), indicating dietary choline or TMAO supplementation, and dietary choline+IMC exposure, each induced significant (permutational multivariate ANOVA, R2=0.49, P=0.001) detectable rearrangements in the overall cecal microbial
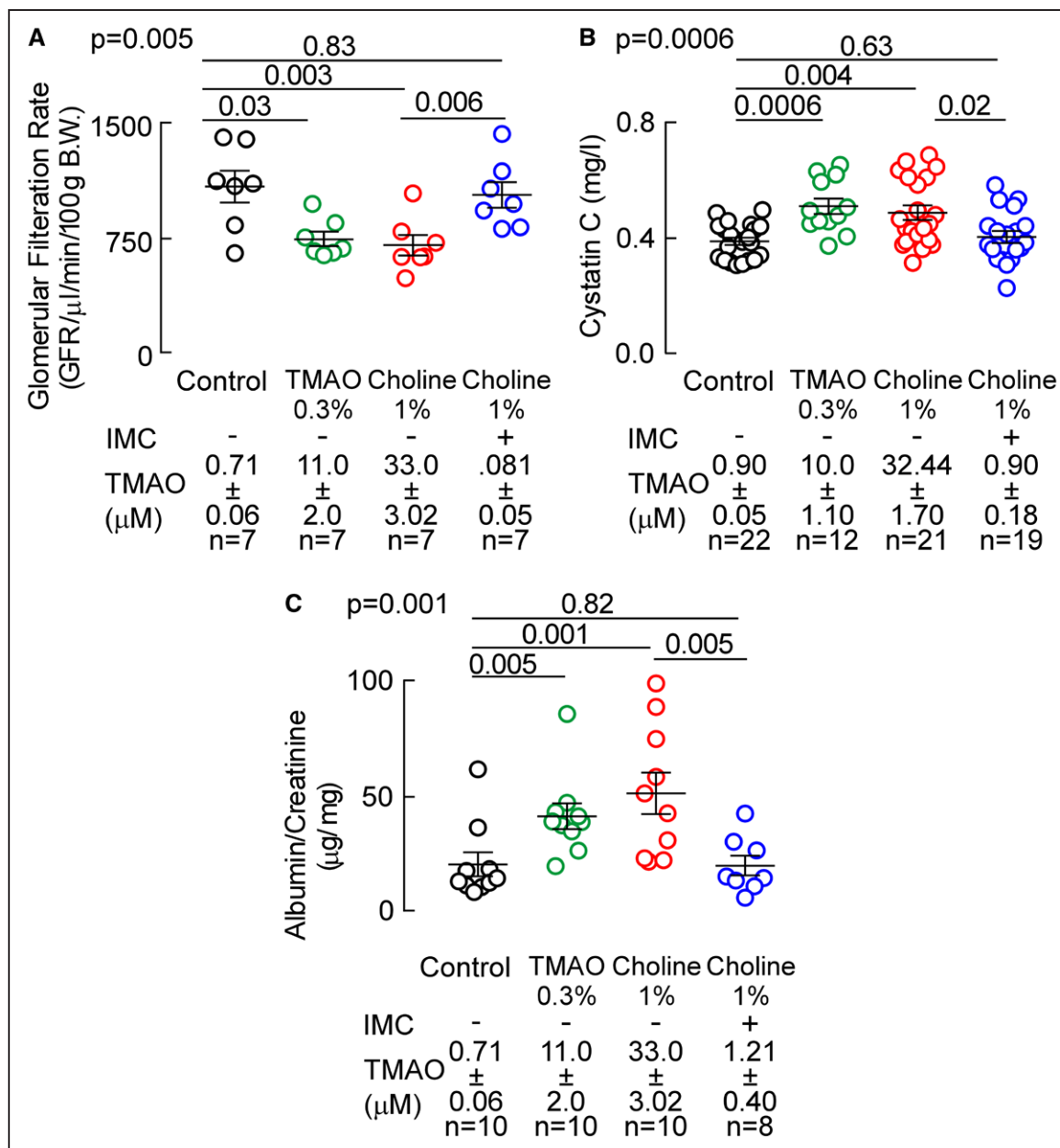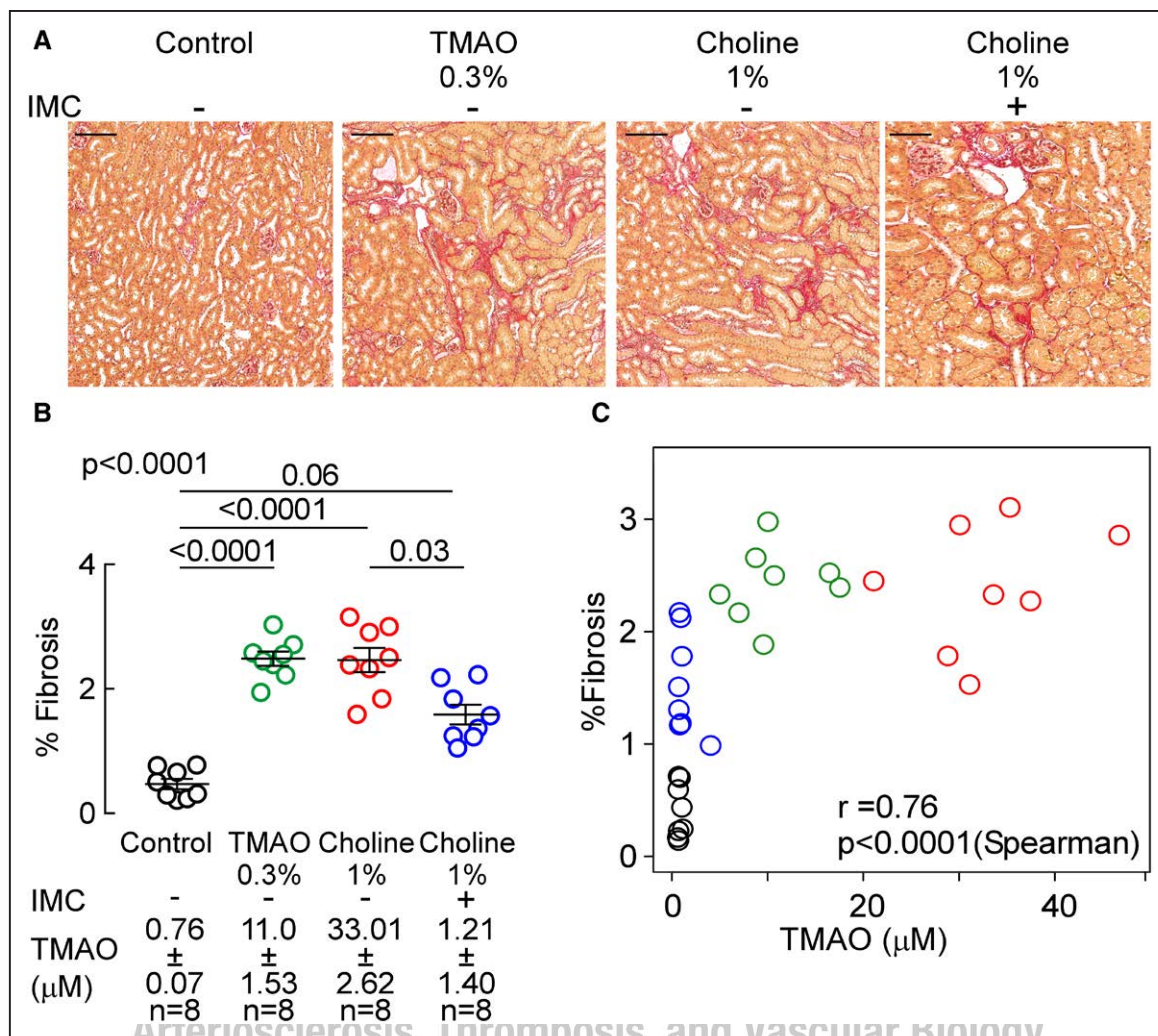
Figure 4. Microbial choline trimethylamine (TMA)-lyase inhibitor iodomethylcholine (IMC) attenuates choline diet-induced renal functional impairment.
A, Glomerular filtration rate (GFR), (**B**) plasma Cystatin C, and (**C**) urinary albumin to creatinine ratio (ACR). Results are presented as mean±SEM. Global *P* value shown was obtained by nonparametric Kruskal-Wallis, and the *P* value among different treatments was determined by nonparametric 1-way ANOVA after Dunn post hoc test.

community. Shannon (which includes evenness) index-based alpha diversity showed significant differences between the different diets (Figure 9B). The control group demonstrated significantly ($P<0.001$) lower alpha diversity in comparison to the other 3 diets (ie, choline, TMAO, and choline+IMC). The addition of IMC to choline treatment significantly reduced the alpha diversity ($P<0.05$), consistent with IMC treatment reversing some of the choline diet–induced community shifts observed. The nonparametric Kruskal-Wallis H-test permitted further identification of 3 cecal microbial taxa whose

proportions accounted for significant ($P<0.05$, BH-FDR corrected) differences observed in the IMC-treated versus non-IMC-treated groups (Figure 9C).

In further analyses, we examined whether the proportions of any of the detected cecal taxa within all groups of mice were significantly correlated with either plasma TMAO levels or markers of renal function and injury, as determined by direct measure of GFR, cystatin C and ACR (Figure I in the Data Supplement). Notably, cecal microbes recovered from the mice fed a high-choline diet showed a significant ($P=4.33\times10^{-4}$) increase in the proportion of

Figure 5. Microbial choline trimethylamine (TMA)-lyase inhibitor iodomethylcholine (IMC) attenuates choline diet-induced renal tubulointerstitial fibrosis.
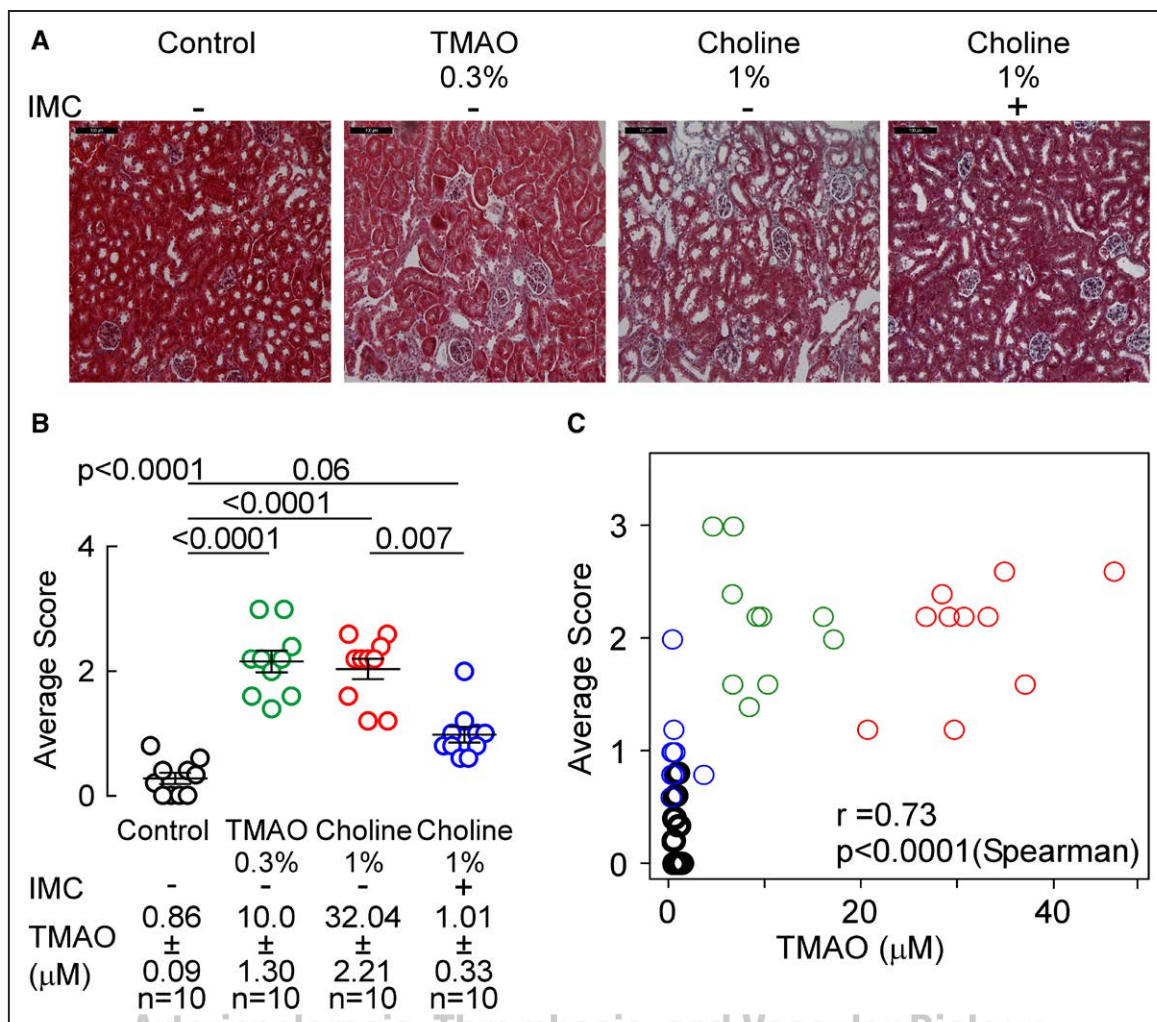**A**, Representative photomicrographs of picrosirius red-stained kidney (scale bar=100 µ), (**B**) fibrosis quantification, and (**C**) correlation between plasma TMA N-oxide (TMAO) and %fibrosis. Results are presented as mean±SEM. Global *P* value shown was obtained by 1-way ANOVA (Kruskal-Wallis), and the *P* value among the different treatments was determined by 1-way ANOVA (Kruskal-Wallis) after Dunn post hoc test and Spearman correlation.

the genus *Lactobacillus,* which further demonstrated positive correlations with TMAO (R^2=0.22), ACR (R^2=0.14) and cystatin C (R^2=0.30), and negative correlations with GFR (R^2=−0.24, Figure 9C; and Figure IA through IC in the Data Supplement). In addition, both TMAO and Choline diets showed reduced proportions of *Bacteroides* compared with control diet, whereas exposure to IMC reversed the proportion of *Bacteroides* to levels observed in mice fed the control diet (P=5.38×10^{-4}, Figure 9C). Furthermore, increased proportions of *Bacteroides* with IMC showed significant negative correlation with plasma TMAO levels (R^2=−0.31, P=0.027; Figure 9D) and with renal functional metrics monitored (cystatin C [R^2=−0.47, P=0.016], ACR [R^2=−0.39, P=1.42×10^{-3}], and positive correlation with GFR [R^2=0.17, P=0.0016]; Figure 9D and Figure IA through IC in the Data Supplement). Moreover, *Lachnospiraceae_UCG-002* showed significant enrichment in

the group supplemented with TMAO and the high-choline diet-fed groups (Figure 9C, P=9.44×10^{-6}), which further showed positive associations with both Cystatin C (R^2=0.52, P=0.034) and ACR (R^2=0.52, P=0.01), and a negative association with GFR (R^2=−0.22, P=3.79×10^{-3}; Figure IA through IC in the Data Supplement). Numerous parallel and directionally relevant correlations between the proportions of *Bacteroides, Lactobacillus,* and *Lachnospiraceae_UCG-002*, and changes in tubulointerstitial fibrosis as monitored via multiple approaches (eg, staining with mason trichrome, picrosirius red or α-SMA) were also observed (Figure IIA through IIC in the Data Supplement).

DISCUSSION

Current treatments to slow progression of CKD and to prevent CKD-related complications, on the whole, are
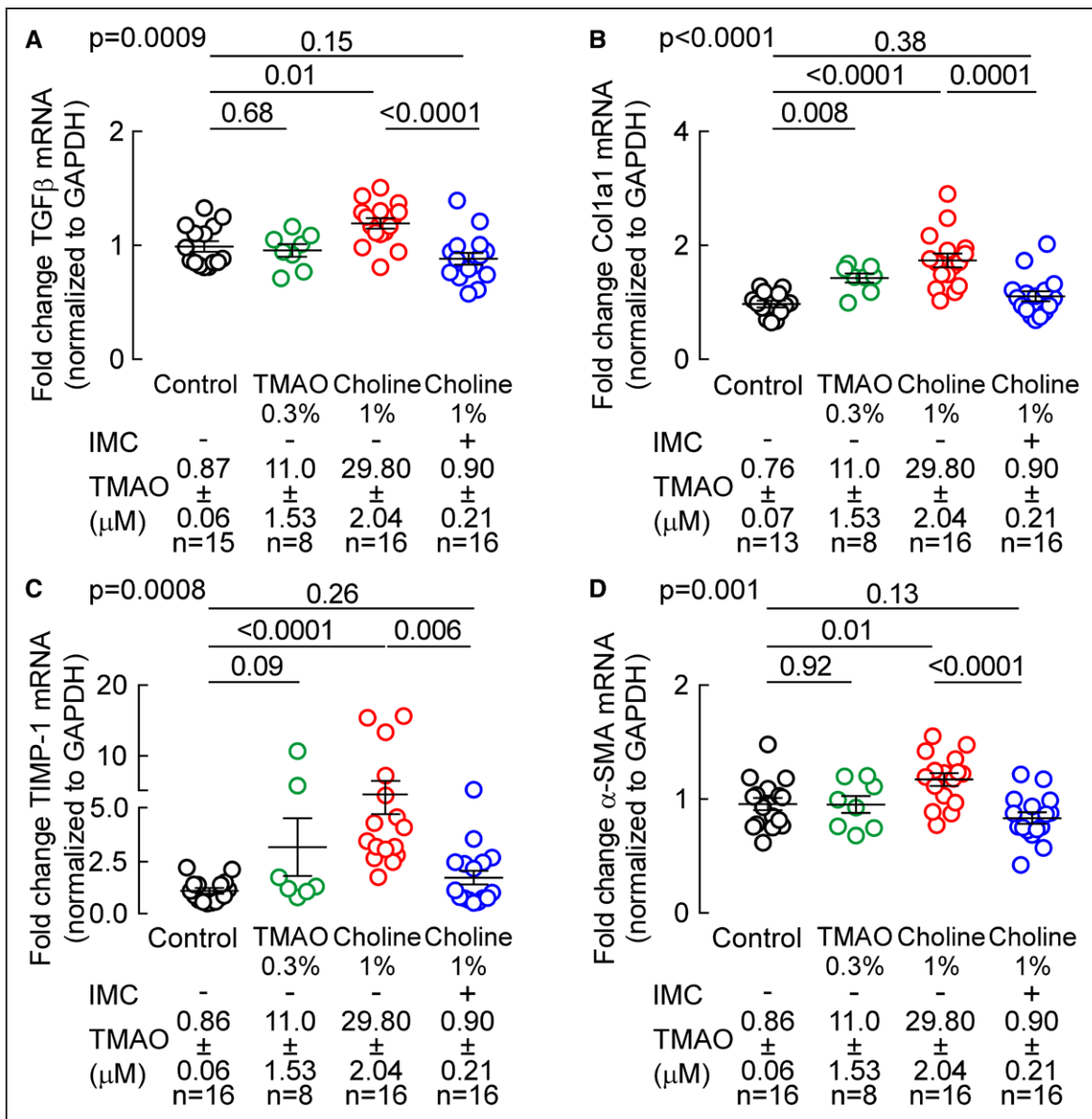
Figure 6. Microbial choline trimethylamine (TMA)-lyase inhibitor iodomethylcholine (IMC) attenuates choline diet-induced renal tubulointerstitial fibrosis.
A, Representative photomicrographs of Masson trichrome-stained (scale bar=100 μ), (**B**) histological scoring of Masson trichrome stained kidneys, and (**C**) correlation between renal histological score and plasma TMA N-oxide (TMAO). Mean scores per mouse±SEM are shown, and global P value was obtained by 1-way ANOVA (Kruskal-Wallis), and the P value among the different treatments was determined by 1-way ANOVA (Kruskal-Wallis) after Dunn post hoc test and Spearman correlation.

limited, and our major treatment strategies are preventative, focusing predominantly on antihypertensive agents.[57,58] Despite these therapies, outcomes in CKD remain poor. Specifically, CKD progression rates remain high and cardiovascular disease remains the major cause of mortality in this at-risk cohort. The present studies suggest that targeting specific gut microbial pathways may prove beneficial for preservation of renal function and represent an exciting new opportunity for further investigations. It is notable that the gut microbiota-dependent TMAO pathway represents a common underlying potential pathogenic process in both CKD and CVD alike. And recent studies show targeting this pathway with nonlethal inhibition of gut microbiota generation of TMA can attenuate atherosclerosis[22] and thrombosis.[23] The present studies extend these observations and suggest that targeting gut microbiota-driven TMA generation, and thus TMAO elevation, may potentially protect against

concurrent heightened cardiovascular disease risks and progression of renal functional decline in CKD subjects.

Recent studies have also shown that dietary interventions (ie, avoidance of red meat) can markedly reduce TMAO levels in subjects.[59] The present studies thus further raise the concept of alternative approaches for dietary management of patients with CKD. Dietary interventions in patients with CKD are an important part of preventive efforts, and in general have suggested minimizing protein intake, in an effort to minimize nitrogenous waste. The present studies suggest a more targeted approach to selectively reduce TMAO levels, while maintaining protein intake, is worth investigation. Sarcopenia and frailty are commonly observed with more advanced stages of renal disease, conditions where maintaining adequate caloric intake and dietary protein is otherwise recommended. Interestingly, in a recent dietary intervention study in subjects with normal renal function,
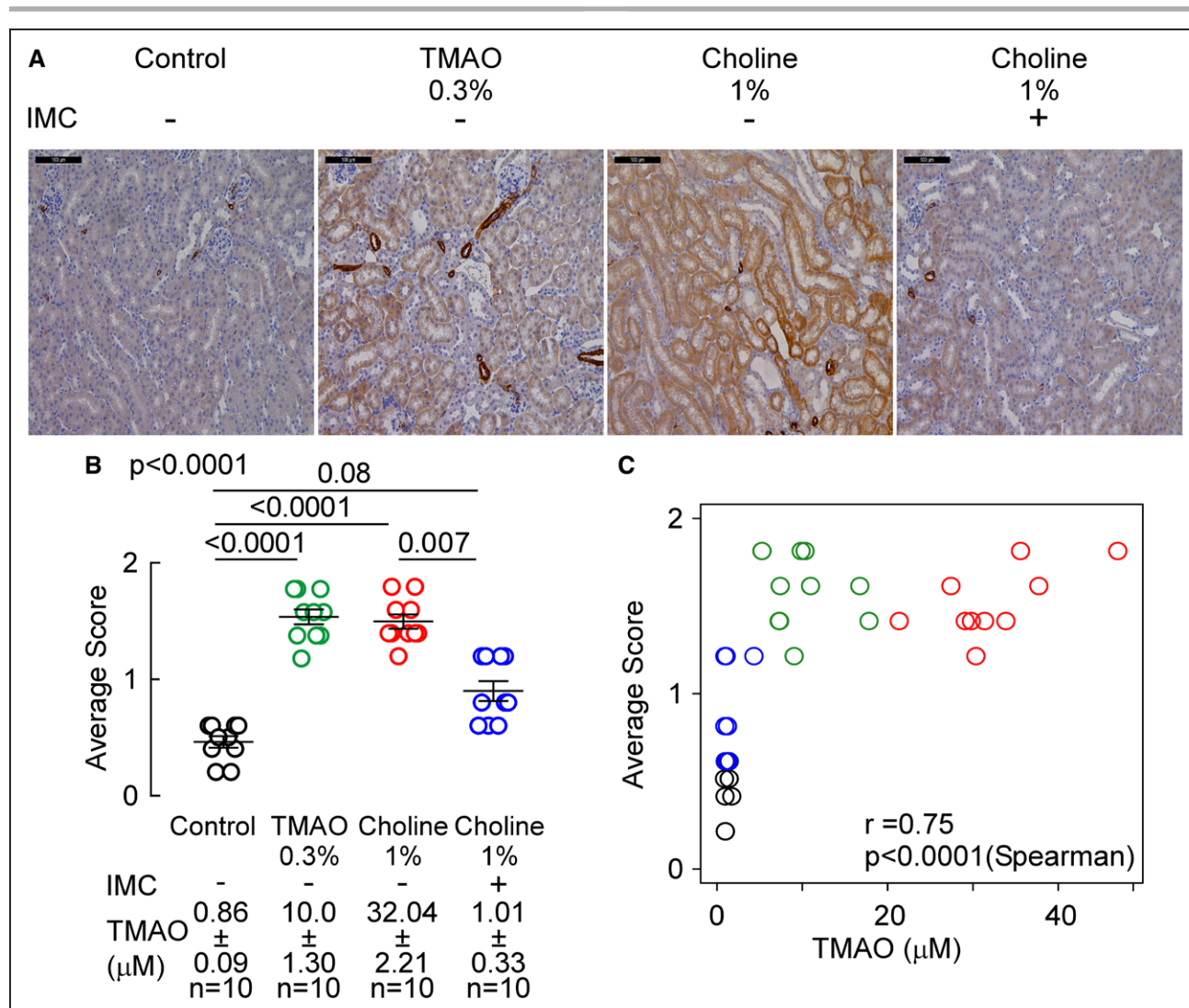
Figure 7. Microbial choline trimethylamine (TMA)-lyase inhibitor iodomethylcholine (IMC) attenuates choline diet-induced renal profibrotic gene expression changes.
Profibrotic gene expression, normalized to GAPDH mRNA transcripts, in murine kidney was analyzed by TaqMan real-time polymerase chain reaction. **A**, TGF-b (transforming growth factor–b), (**B**) Col1a1 (α-1-type1 collagen), (**C**) TIMP-1 (tissue inhibitor of metalloproteinase 1) gene expression, and (**D**) α-SMA (smooth muscle actin). Results are presented as mean±SEM. Global *P* value shown was obtained by nonparametric Kruskal-Wallis, and the *P* value among different treatments was determined by nonparametric 1-way ANOVA after Dunn post hoc test.

chronic change in protein source (eg, red meat versus white meat or vegetarian) while maintaining isocaloric diets was shown to substantially impacted TMAO levels through several mechanisms. The red meat-rich diet markedly increased TMAO levels due to enhanced density of TMAO precursors, but also by both eliciting substantial changes in gut microbial community functional output of TMA (enhanced conversion of carnitine into TMAO), and lowering the fractional renal excretion of TMAO.[59] Thus, chronic exposure to a diet rich in red meat led to less efficient TMAO excretion, which was reversed by the white meat and nonmeat diets.[59] In alternative recent studies, it was reported that a short-term significant increase in the daily protein allowance was associated with increased circulating TMAO levels.[60] The precise choice of protein source can thus have a significant impact on TMAO production and excretion, and further studies seem warranted to determine if differing sources of dietary protein can significantly impact long-term renal function changes in subjects with CKD.

The prevalence of CKD is increasing as the population both ages and becomes increasing obese (thereby
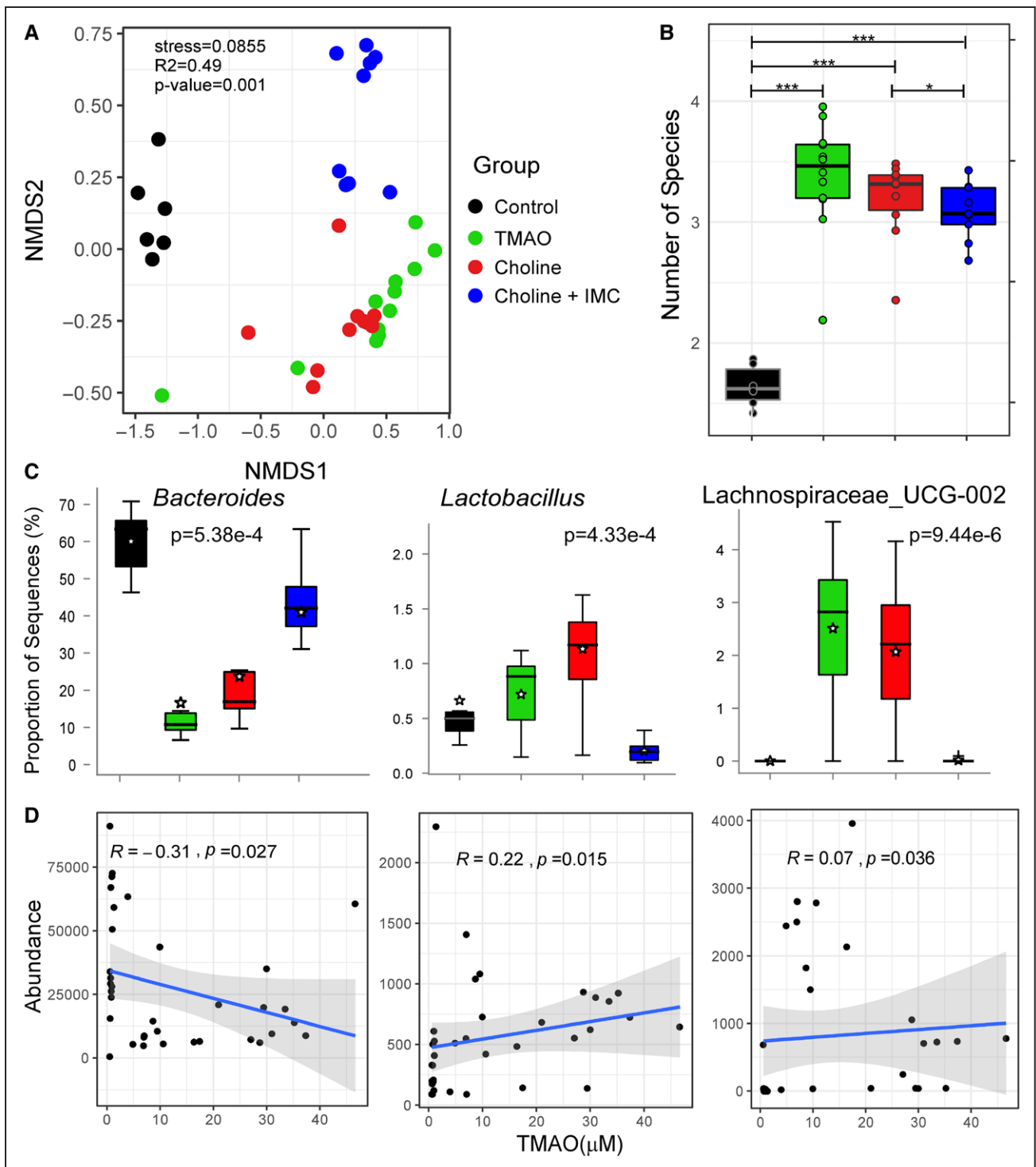
Figure 8. Microbial choline trimethylamine (TMA)-lyase inhibitor iodomethylcholine (IMC) attenuates choline diet-induced α-SMA (α-smooth muscle actin) protein expression.
A, Representative α-SMA renal immunohistochemistry pictographs (scale bar=100 μ), (**B**) α-SMA protein levels score, and (**C**) plasma TMA N-oxide (TMAO) levels correlation with prevalence of α-SMA staining. Results are presented as mean±SEM. Global *P* value shown was obtained by nonparametric Kruskal-Wallis, and the *P* value among different treatments was determined by nonparametric 1-way ANOVA after Dunn post hoc test. For correlation between plasma TMAO levels and α-SMA staining, *P* values were calculated using nonparametric Spearman correlation.

increasing the prevalence of diabetes mellitus).[61] Elevated plasma TMAO levels in patients with CKD are associated with higher rates of adverse CVD events and mortality. Moreover, elevated levels of both TMAO and choline are associated with enhanced progressive loss of renal function and development of CKD.[1,18,19,21,62–64] It should also be noted, however, that not all published clinical studies on TMAO have reported a significant positive association with CVD risks. While adverse prognostic value for TMAO is observed in many CKD cohorts,[1,18,19,62–65] in maintenance hemodialysis populations the incremental prognostic value of TMAO has at times not been clearly demonstrated, suggesting either the smaller size of some of these studies, or a possible plateau effect maybe observed when virtually all members

of the cohort examined have high TMAO level (ie, even the lowest quartile have markedly elevated TMAO levels and further increases in risk may not be observed with further elevations in TMAO).[14,66–68] There have been multiple recent meta-analyses that have extensively examined the clinical association between TMAO and both incident CVD risks and mortality—all of the published meta-analyses thus far report a significant positive association with increasing TMAO levels independent of traditional CVD risk factors and renal status.[62,69,70] In one meta-analysis, each 10 μmol/L change in TMAO level was associated with an ≈7.4% increase in mortality rate.[62] It is also notable that a recent clinical investigation in subjects with ESRD on maintenance hemodialysis report that TMAO has a smaller volume of

Figure 9. Trimethylamine (TMA)-lyase inhibitor, iodomethylcholine (IMC), impacts the choline diet-induced changes in cecal microbial community associated with plasma TMA N-oxide (TMAO) levels.
A, The nonmetric multidimensional scaling plots (NMDS) based on Bray-Curtis index between the cecal microbiota of mice treated with indicated diets, that is, Control, TMAO, Choline, and Choline+IMC samples. Each data point represents a sample from a distinct mouse. Statistical analysis was performed using permutational multivariate ANOVA, and *P* values are labeled in the plots. R2 values are also mentioned for comparisons with significant *P* values. The R2 values stand for % variance explained by the variable of interest, that is, diet. **B**, Boxplots of Shannon diversity indices distinguishing Control, TMAO, Choline, and Choline+IMC samples. Statistical analysis was performed using paired *t* tests. Plotted are interquartile ranges (boxes), and the dark line in the box is the median. ***Stands for $P \leq 0.001$ and *Stands for *P* value <0.05. **C**, Multi-group Kruskal-Wallis H-test showing results for statistically significant (BH-FDR $P < 0.05$) genera differentiating 4 groups, that is, Control, TMAO, Choline, and Choline+IMC. **D**, Linear regression-based scatter plots showing correlation between abundance of select taxa and TMAO (µmol/L) levels. The R2 and *P* values are plotted within each panel.

distribution than urea and is cleared better than urea by the kidney. In addition to its dialyzability compared with other more tightly protein-bound uremic toxins, this has led to the suggestion that additional strategies in ESRD, such as reducing production coupled with more frequent dialysis, might also help to reduce TMAO levels in ESRD subjects.[71]

It is also notable that the present small molecule inhibitor used, IMC, was specifically developed to be nonlethal (ie, unlike an antibiotic) and thus should exert less selective pressure for development of gut microbial resistance. Moreover, the capacity of the inhibitor to accumulate within gut microbiota in vivo was previously developed based on the recognition that upon inhibiting catalysis of choline within the microbe, the bacterial cytosolic levels will accumulate, be sensed as an abundant carbon fuel source, and the entire *cutC* gene cluster,[72,73] including the bacterial choline transporter,[23] could then be upregulated. Thus, the more effective the inhibitor is at blocking choline catabolism, the greater the microbe accumulates both IMC and choline (both of which were noted in the present studies to be highly enriched within the gut luminal contents, which are predominantly comprised of gut bacteria). This has the functional outcome of sequestering choline from the gut luminal extracellular space, depriving other microbial community members from choline. Thus, as long as a significant enough proportion of microbes within the community are sufficiently inhibited, depletion of intestinal luminal choline will suppress colon gut microbial community output of TMA (and thus host production of TMAO), a process that would be more resilient to development of resistance.

The present studies add to the growing body of evidence mechanistically linking gut microbiota-generated TMA/TMAO to multiple indices of renal functional impairment and fibrosis. They also suggest that further studies exploring the link between TMAO levels and risk for glomerular and tubular injury in subjects are needed. Renal fibrosis, a consequence of an excessive accumulation of extracellular matrix, represents a relatively late and common manifestation of nearly all chronic and progressive nephropathies.[58] It is thus of interest that elevated gut microbiota-driven plasma TMAO levels appear to directly contribute to enhanced fibrosis in this mouse model, where multiple different indices of fibrosis were quantitatively examined (ie, histological staining procedures and profibrotic gene expression changes, protein levels). Whether nonlethal gut microbiota-targeting inhibitors that suppress TMAO levels represent a new renal-sparing therapy in some subjects with CKD awaits further investigation.

Several limitations of the present study warrant consideration. Most notably, not all CKD will be driven by TMAO-dependent mechanisms. While CKD is associated with elevated TMAO levels, not all subjects with CKD have elevated TMAO. Thus, one could imagine a gut microbe-targeted TMA-lyase inhibitor to be used with the companion diagnostic TMAO test, as inhibition of this pathway would be more likely to show benefit among subjects with heightened TMAO levels. In addition, the effect of reducing TMAO on CKD progression rate in humans remains to be evaluated. Moreover, while the present studies have demonstrated that inhibiting TMAO production can prevent both renal functional impairment and fibrosis, they have not examined if reduction in TMAO with established renal disease can either halt the progression of, or foster regression in, renal functional decline and adverse remodeling. Finally, beyond the induction of multiple profibrotic gene expression changes, the present studies do not examine the molecular mechanisms by which TMAO exerts its adverse effects on renal functional impairment and fibrosis. Notably, a recent study by Chen et al[74] reported the discovery of the endoplasmic reticulum stress kinase PERK (EIF2AK3) as a TMAO receptor for glucose-related metabolic effects associated with the metabolite. It remains unknown if PERK participates in TMAO-driven renal function decline or if TMAO is acting via other proposed mechanisms, such as an alternate (still un-identified) receptor or via demonstrated effect on protein conformation and stability.[75,76]

In conclusion, the present studies provide further evidence in support of a gut microbial contribution to renal function decline and adverse remodeling in a chronic sympathetic-driven isoproterenol infusion model of CKD. More significantly, the results indicate that targeting TMAO metabolism may represent a potential therapeutic approach for preventing or retarding CKD development and progression, while concurrently reducing adverse cardiovascular events associated with TMAO elevation. Moving beyond TMAO, one can also envision multiple potential gut microbiota-generated uremic toxins[77] as potential additional candidates for therapeutic intervention and investigation.

ARTICLE INFORMATION

REFERENCES

1. Tang WH, Wang Z, Kennedy DJ, Wu Y, Buffa JA, Agatisa-Boyle B, Li XS, Levison BS, Hazen SL. Gut microbiota-dependent trimethylamine N-oxide (TMAO) pathway contributes to both development of renal insufficiency and mortality risk in chronic kidney disease. *Circ Res*. 2015;116:448–455. doi: 10.1161/CIRCRESAHA.116.305360

2. Wong J, Piceno YM, DeSantis TZ, Pahl M, Andersen GL, Vaziri ND. Expansion of urease- and uricase-containing, indole- and p-cresol-forming and contraction of short-chain fatty acid-producing intestinal microbiota in ESRD. *Am J Nephrol*. 2014;39:230–237. doi: 10.1159/000360010

3. Strid H, Simrén M, Stotzer PO, Ringström G, Abrahamsson H, Björnsson ES. Patients with chronic renal failure have abnormal small intestinal motility and a high prevalence of small intestinal bacterial overgrowth. *Digestion*. 2003;67:129–137. doi: 10.1159/000071292

4. Vaziri ND, Wong J, Pahl M, Piceno YM, Yuan J, DeSantis TZ, Ni Z, Nguyen TH, Andersen GL. Chronic kidney disease alters intestinal microbial flora. *Kidney Int*. 2013;83:308–315. doi: 10.1038/ki.2012.345

5. Simenhoff ML, Saukkonen JJ, Burke JF, Wesson LG, Schaedler RW. Amine metabolism and the small bowel in uraemia. *Lancet*. 1976;2:818–821. doi: 10.1016/s0140-6736(76)91207-1

6. Barrios C, Beaumont M, Pallister T, Villar J, Goodrich JK, Clark A, Pascual J, Ley RE, Spector TD, Bell JT, et al. Gut-microbiota-metabolite axis in early renal function decline. *PLoS One*. 2015;10:e0134311. doi: 10.1371/journal.pone.0134311

7. Kikuchi M, Ueno M, Itoh Y, Suda W, Hattori M. Uremic toxin-producing gut microbiota in rats with chronic kidney disease. *Nephron*. 2017;135:51–60. doi: 10.1159/000450619

8. Mishima E, Fukuda S, Mukawa C, Yuri A, Kanemitsu Y, Matsumoto Y, Akiyama Y, Fukuda NN, Tsukamoto H, Asaji K, et al. Evaluation of the impact of gut microbiota on uremic solute accumulation by a CE-TOFMS-based metabolomics approach. *Kidney Int*. 2017;92:634–645. doi: 10.1016/j.kint.2017.02.011

9. Sun CY, Chang SC, Wu MS. Uremic toxins induce kidney fibrosis by activating intrarenal renin-angiotensin-aldosterone system associated epithelial-to-mesenchymal transition. *PLoS One*. 2012;7:e34026. doi: 10.1371/journal.pone.0034026

10. Watanabe H, Miyamoto Y, Honda D, Tanaka H, Wu Q, Endo M, Noguchi T, Kadowaki D, Ishima Y, Kotani S, et al. p-Cresyl sulfate causes renal tubular cell damage by inducing oxidative stress by activation of NADPH oxidase. *Kidney Int*. 2013;83:582–592. doi: 10.1038/ki.2012.448

11. Sun CY, Chang SC, Wu MS. Suppression of klotho expression by protein-bound uremic toxins is associated with increased DNA methyltransferase expression and DNA hypermethylation. *Kidney Int*. 2012;81:640–650. doi: 10.1038/ki.2011.445

12. Meijers BK, Claes K, Bammens B, de Loor H, Viaene L, Verbeke K, Kuypers D, Vanrenterghem Y, Evenepoel P. p-Cresol and cardiovascular risk in mild-to-moderate kidney disease. *Clin J Am Soc Nephrol*. 2010;5:1182–1189. doi: 10.2215/CJN.07971109

13. Basile C, Libutti P, Di Turo AL, Casino FG, Vernaglione L, Tundo S, Maselli P, De Nicolò EV, Ceci E, Teutonico A, et al. Removal of uraemic retention solutes in standard bicarbonate haemodialysis and long-hour slow-flow bicarbonate haemodialysis. *Nephrol Dial Transplant*. 2011;26:1296–1303. doi: 10.1093/ndt/gfq543

14. Kalim S, Wald R, Yan AT, Goldstein MB, Kiaii M, Xu D, Berg AH, Clish C, Thadhani R, Rhee EP, et al. Extended duration nocturnal hemodialysis and changes in plasma metabolite profiles. *Clin J Am Soc Nephrol*. 2018;13:436–444. doi: 10.2215/CJN.08790817

15. Wang IK, Wu YY, Yang YF, Ting IW, Lin CC, Yen TH, Chen JH, Wang CH, Huang CC, Lin HC. The effect of probiotics on serum levels of cytokine and endotoxin in peritoneal dialysis patients: a randomised, double-blind, placebo-controlled trial. *Benef Microbes*. 2015;6:423–430. doi: 10.3920/BM2014.0088

16. Viramontes-Hörner D, Márquez-Sandoval F, Martín-del-Campo F, Vizmanos-Lamotte B, Sandoval-Rodríguez A, Armendáriz-Borunda J, García-Bejarano H, Renoirte-López K, García-García G. Effect of a symbiotic gel (Lactobacillus acidophilus + Bifidobacterium lactis + inulin) on presence and severity of gastrointestinal symptoms in hemodialysis patients. *J Ren Nutr*. 2015;25:284–291. doi: 10.1053/j.jrn.2014.09.008

17. Weir MR, Bakris GL, Bushinsky DA, Mayo MR, Garza D, Stasiv Y, Wittes J, Christ-Schmidt H, Berman L, Pitt B; OPAL-HK Investigators. Patiromer in patients with kidney disease and hyperkalemia receiving RAAS inhibitors. *N Engl J Med*. 2015;372:211–221. doi: 10.1056/NEJMoa1410853

18. Kim RB, Morse BL, Djurdjev O, Tang M, Muirhead N, Barrett B, Holmes DT, Madore F, Clase CM, Rigatto C, et al; CanPREDDICT Investigators. Advanced chronic kidney disease populations have elevated trimethylamine N-oxide levels associated with increased cardiovascular events. *Kidney Int*. 2016;89:1144–1152. doi: 10.1016/j.kint.2016.01.014

19. Missailidis C, Hällqvist J, Qureshi AR, Barany P, Heimbürger O, Lindholm B, Stenvinkel P, Bergman P. Serum trimethylamine-N-oxide is strongly related to renal function and predicts outcome in chronic kidney disease. *PLoS One*. 2016;11:e0141738. doi: 10.1371/journal.pone.0141738

20. Zhu W, Wang Z, Tang WHW, Hazen SL. Gut microbe-generated trimethylamine N-oxide from dietary choline is prothrombotic in subjects. *Circulation*. 2017;135:1671–1673. doi: 10.1161/CIRCULATIONAHA.116.025338

21. Rhee EP, Clish CB, Ghorbani A, Larson MG, Elmariah S, McCabe E, Yang Q, Cheng S, Pierce K, Deik A, et al. A combined epidemiologic and metabolomic approach improves CKD prediction. *J Am Soc Nephrol*. 2013;24:1330–1338. doi: 10.1681/ASN.2012101006

22. Wang Z, Roberts AB, Buffa JA, Levison BS, Zhu W, Org E, Gu X, Huang Y, Zamanian-Daryoush M, Culley MK, et al. Non-lethal inhibition of gut microbial trimethylamine production for the treatment of atherosclerosis. *Cell*. 2015;163:1585–1595. doi: 10.1016/j.cell.2015.11.055

23. Roberts AB, Gu X, Buffa JA, Hurd AG, Wang Z, Zhu W, Gupta N, Skye SM, Cody DB, Levison BS, et al. Development of a gut microbe-targeted non-lethal therapeutic to inhibit thrombosis potential. *Nat Med*. 2018;24:1407–1417. doi: 10.1038/s41591-018-0128-1

24. Dubey RK, Gillespie DG, Keller PJ, Imthurn B, Zacharia LC, Jackson EK. Role of methoxyestradiols in the growth inhibitory effects of estradiol on human glomerular mesangial cells. *Hypertension*. 2002;39(2 pt 2):418–424. doi: 10.1161/hy0202.103297

25. Matsuda T, Yamamoto T, Muraguchi A, Saatcioglu F. Cross-talk between transforming growth factor-beta and estrogen receptor signaling through Smad3. *J Biol Chem*. 2001;276:42908–42914. doi: 10.1074/jbc.M105316200

26. Mankhey RW, Bhatti F, Maric C. 17beta-Estradiol replacement improves renal function and pathology associated with diabetic nephropathy. *Am J Physiol Renal Physiol*. 2005;288:F399–F405. doi: 10.1152/ajprenal.00195.2004

27. Long DA, Kolatsi-Joannou M, Price KL, Dessapt-Baradez C, Huang JL, Papakrivopoulou E, Hubank M, Korstanje R, Gnudi L, Woolf AS. Albuminuria is associated with too few glomeruli and too much testosterone. *Kidney Int*. 2013;83:1118–1129. doi: 10.1038/ki.2013.45

28. Wang Z, Klipfell E, Bennett BJ, Koeth R, Levison BS, Dugar B, Feldstein AE, Britt EB, Fu X, Chung YM, et al. Gut flora metabolism of phosphatidylcholine promotes cardiovascular disease. *Nature*. 2011;472:57–63. doi: 10.1038/nature09922

29. Wang Z, Levison BS, Hazen JE, Donahue L, Li XM, Hazen SL. Measurement of trimethylamine-N-oxide by stable isotope dilution liquid chromatography tandem mass spectrometry. *Anal Biochem*. 2014;455:35–40. doi: 10.1016/j.ab.2014.03.016

30. Scarfe L, Schock-Kusch D, Ressel L, Friedemann J, Shulhevich Y, Murray P, Wilm B, de Caestecker M. Transdermal measurement of glomerular filtration rate in mice. *J Vis Exp*. 2018;140:58520. doi: 10.3791/58520

31. Schreiber A, Shulhevich Y, Geraci S, Hesser J, Stsepankou D, Neudecker S, Koenig S, Heinrich R, Hoecklin F, Pill J, et al. Transcutaneous measurement of renal function in conscious mice. *Am J Physiol Renal Physiol*. 2012;303:F783–F788. doi: 10.1152/ajprenal.00279.2012

32. Schock-Kusch D, Xie Q, Shulhevich Y, Hesser J, Stsepankou D, Sadick M, Koenig S, Hoecklin F, Pill J, Gretz N. Transcutaneous assessment of renal function in conscious rats with a device for measuring FITC-sinistrin disappearance curves. *Kidney Int*. 2011;79:1254–1258. doi: 10.1038/ki.2011.31

33. Huttenhower C, Gevers D, Knight R, Abubucker S, Badger JH, Chinwalla AT, Creasy HH, Earl AM, FitzGerald MG, Fulton RS, et al; Human Microbiome

Project Consortium. Structure, function and diversity of the healthy human microbiome. *Nature*. 2012;486:207–214. doi: 10.1038/nature11234

34. Caporaso JG, Kuczynski J, Stombaugh J, Bittinger K, Bushman FD, Costello EK, Fierer N, Peña AG, Goodrich JK, Gordon JI, et al. QIIME allows analysis of high-throughput community sequencing data. *Nat Methods*. 2010;7:335–336. doi: 10.1038/nmeth.f.303

35. Callahan BJ, McMurdie PJ, Rosen MJ, Han AW, Johnson AJ, Holmes SP. DADA2: High-resolution sample inference from Illumina amplicon data. *Nat Methods*. 2016;13:581–583. doi: 10.1038/nmeth.3869

36. McMurdie PJ, Holmes S. phyloseq: an R package for reproducible interactive analysis and graphics of microbiome census data. *PLoS One*. 2013;8:e61217. doi: 10.1371/journal.pone.0061217

37. McMurdie PJ, Holmes S. Waste not, want not: why rarefying microbiome data is inadmissible. *PLoS Comput Biol*. 2014;10:e1003531. doi: 10.1371/journal.pcbi.1003531

38. Wickham H. *ggplot2: Elegant Graphics for Data Analysis*. Springer Publishing Company, Incorporated; 2009.

39. Benjamini Y. Discovering the false discovery rate. *J R Stat Soc Series B Stat Methodol*. 2010;72:405–416.

40. Tiit EM. Nonparametric statistical methods. Myles Hollander and Douglas A. Wolfe, Wiley, Chichester, 1999. ISBN 0-471-19045-4. *Stat Med*. 2000;19:1386–1388.

41. Schlaich MP, Socratous F, Hennebry S, Eikelis N, Lambert EA, Straznicky N, Esler MD, Lambert GW. Sympathetic activation in chronic renal failure. *J Am Soc Nephrol*. 2009;20:933–939. doi: 10.1681/ASN.2008040402

42. Zoccali C, Mallamaci F, Parlongo S, Cutrupi S, Benedetto FA, Tripepi G, Bonanno G, Rapisarda F, Fatuzzo P, Seminara G, et al. Plasma norepinephrine predicts survival and incident cardiovascular events in patients with end-stage renal disease. *Circulation*. 2002;105:1354–1359. doi: 10.1161/hc1102.105261

43. de Ponte MC, Casare FAM, Costa-Pessoa JM, Cardoso VG, Malnic G, Mello-Aires M, Volpini RA, Thieme K, Oliveira-Souza M. The role of β-adrenergic overstimulation in the early stages of renal injury. *Kidney Blood Press Res*. 2017;42:1277–1289. doi: 10.1159/000485931

44. Grassi G, Quarti-Trevano F, Seravalle G, Arenare F, Volpe M, Furiani S, Dell'Oro R, Mancia G. Early sympathetic activation in the initial clinical stages of chronic renal failure. *Hypertension*. 2011;57:846–851. doi: 10.1161/HYPERTENSIONAHA.110.164780

45. Amann K, Rump LC, Simonaviciene A, Oberhauser V, Wessels S, Orth SR, Gross ML, Koch A, Bielenberg GW, Van Kats JP, et al. Effects of low dose sympathetic inhibition on glomerulosclerosis and albuminuria in subtotally nephrectomized rats. *J Am Soc Nephrol*. 2000;11:1469–1478.

46. Vonend O, Marsalek P, Russ H, Wulkow R, Oberhauser V, Rump LC. Moxonidine treatment of hypertensive patients with advanced renal failure. *J Hypertens*. 2003;21:1709–1717. doi: 10.1097/00004872-200309000-00021

47. Zheng G, Cai J, Chen X, Chen L, Ge W, Zhou X, Zhou H. Relaxin ameliorates renal fibrosis and expression of endothelial cell transition markers in rats of isoproterenol-induced heart failure. *Biol Pharm Bull*. 2017;40:960–966. doi: 10.1248/bpb.b16-00882

48. Liu Q, Zhang Q, Wang K, Wang S, Lu D, Li Z, Geng J, Fang P, Wang Y, Shan Q. Renal denervation findings on cardiac and renal fibrosis in rats with isoproterenol induced cardiomyopathy. *Sci Rep*. 2015;5:18582. doi: 10.1038/srep18582

49. Ide S, Yamamoto R, Takeda H, Minami M. Bidirectional brain-gut interactions: Involvement of noradrenergic transmission within the ventral part of the bed nucleus of the stria terminalis. *Neuropsychopharmacol Rep*. 2018;38:37–43. doi: 10.1002/npr2.12004

50. Thollander M, Svensson TH, Hellström PM. Stimulation of beta-adrenoceptors with isoprenaline inhibits small intestinal activity fronts and induces a postprandial-like motility pattern in humans. *Gut*. 1997;40:376–380. doi: 10.1136/gut.40.3.376

51. Morris AI, Turnberg LA. Influence of isoproterenol and propranolol on human intestinal transport in vivo. *Gastroenterology*. 1981;81:1076–1079.

52. Gáti T, Gelencsér F, Hideg J. The role of adrenergic receptors in the regulation of gastric motility in the rat. *Z Exp Chir*. 1975;8:179–184.

53. Sorribas M, de Gottardi A, Moghadamrad S, Hassan M, Spadoni I, Rescigno M, Wiest R. Isoproterenol disrupts intestinal barriers activating gut-liver-axis: effects on intestinal mucus and vascular barrier as entry sites. *Digestion*. 2019:1–13. doi: 10.1159/000502112

54. Chothani S, Schäfer S, Adami E, Viswanathan S, Widjaja AA, Langley SR, Tan J, Wang M, Quaife NM, Jian Pua C, et al. Widespread translational control of fibrosis in the human heart by RNA-binding proteins. *Circulation*. 2019;140:937–951. doi: 10.1161/CIRCULATIONAHA.119.039596

55. Zhang A, Liu X, Cogan JG, Fuerst MD, Polikandriotis JA, Kelm RJ Jr, Strauch AR. YB-1 coordinates vascular smooth muscle alpha-actin gene activation by transforming growth factor beta1 and thrombin during differentiation of human pulmonary myofibroblasts. *Mol Biol Cell*. 2005;16:4931–4940. doi: 10.1091/mbc.e05-03-0216

56. Strauch AR, Hariharan S. Dynamic interplay of smooth muscle α-actin gene-regulatory proteins reflects the biological complexity of myofibroblast differentiation. *Biology (Basel)*. 2013;2:555–586. doi: 10.3390/biology2020555

57. Nelson RG, Tuttle KR, Bilous RW, Gonzalez-Campoy JM, Mauer M, Molitch ME, Sharma K, Fradkin JE, Narva AS, Wilt TJ, et al; National Kidney Foundation. KDOQI clinical practice guideline for diabetes and CKD: 2012 update. *Am J Kidney Dis*. 2012;60:850–886. doi: 10.1053/j.ajkd.2012.07.005

58. Humphreys BD. Mechanisms of renal fibrosis. *Annu Rev Physiol*. 2018;80:309–326. doi: 10.1146/annurev-physiol-022516-034227

59. Wang Z, Bergeron N, Levison BS, Li XS, Chiu S, Jia X, Koeth RA, Li L, Wu Y, Tang WHW, et al. Impact of chronic dietary red meat, white meat, or non-meat protein on trimethylamine N-oxide metabolism and renal excretion in healthy men and women. *Eur Heart J*. 2019;40:583–594. doi: 10.1093/eurheartj/ehy799

60. Mitchell SM, Milan AM, Mitchell CJ, Gillies NA, D'Souza RF, Zeng N, Ramzan F, Sharma P, Knowles SO, Roy NC, et al. Protein intake at twice the RDA in older men increases circulatory concentrations of the microbiome metabolite trimethylamine-N-oxide (TMAO). *Nutrients*. 2019;11:E2207. doi: 10.3390/nu11092207

61. Coresh J, Astor BC, Greene T, Eknoyan G, Levey AS. Prevalence of chronic kidney disease and decreased kidney function in the adult US population: third national health and nutrition examination survey. *Am J Kidney Dis*. 2003;41:1–12. doi: 10.1053/ajkd.2003.50007

62. Schiattarella GG, Sannino A, Toscano E, Giugliano G, Gargiulo G, Franzone A, Trimarco B, Esposito G, Perrino C. Gut microbe-generated metabolite trimethylamine-N-oxide as cardiovascular risk biomarker: a systematic review and dose-response meta-analysis. *Eur Heart J*. 2017;38:2948–2956. doi: 10.1093/eurheartj/ehx342

63. Stubbs JR, House JA, Ocque AJ, Zhang S, Johnson C, Kimber C, Schmidt K, Gupta A, Wetmore JB, Nolin TD, et al. Serum trimethylamine-N-oxide is elevated in CKD and correlates with coronary atherosclerosis burden. *J Am Soc Nephrol*. 2016;27:305–313. doi: 10.1681/ASN.2014111063

64. Robinson-Cohen C, Newitt R, Shen DD, Rettie AE, Kestenbaum BR, Himmelfarb J, Yeung CK. Association of FMO3 variants and trimethylamine N-oxide concentration, disease progression, and mortality in CKD patients. *PLoS One*. 2016;11:e0161074. doi: 10.1371/journal.pone.0161074

65. Gruppen EG, Garcia E, Connelly MA, Jeyarajah EJ, Otvos JD, Bakker SJL, Dullaart RPF. TMAO is associated with mortality: impact of modestly impaired renal function. *Sci Rep*. 2017;7:13781. doi: 10.1038/s41598-017-13739-9

66. Kaysen GA, Johansen KL, Chertow GM, Dalrymple LS, Kornak J, Grimes B, Dwyer T, Chassy AW, Fiehn O. Associations of trimethylamine N-oxide with nutritional and inflammatory biomarkers and cardiovascular outcomes in patients new to dialysis. *J Ren Nutr*. 2015;25:351–356. doi: 10.1053/j.jrn.2015.02.006

67. Stubbs JR, Stedman MR, Liu S, Long J, Franchetti Y, West RE 3rd, Prokopienko AJ, Mahnken JD, Chertow GM, Nolin TD. Trimethylamine N-oxide and cardiovascular outcomes in patients with ESKD receiving maintenance hemodialysis. *Clin J Am Soc Nephrol*. 2019;14:261–267. doi: 10.2215/CJN.06190518

68. Shafi T, Powe NR, Meyer TW, Hwang S, Hai X, Melamed ML, Banerjee T, Coresh J, Hostetter TH. Trimethylamine N-oxide and cardiovascular events in hemodialysis patients. *J Am Soc Nephrol*. 2017;28:321–331. doi: 10.1681/ASN.2016030374

69. Heianza Y, Ma W, Manson JE, Rexrode KM, Qi L. Gut microbiota metabolites and risk of major adverse cardiovascular disease events and death: a systematic review and meta-analysis of prospective studies. *J Am Heart Assoc*. 2017;6:e004947. doi: 10.1161/JAHA.116.004947

70. Qi J, You T, Li J, Pan T, Xiang L, Han Y, Zhu L. Circulating trimethylamine N-oxide and the risk of cardiovascular diseases: a systematic review and meta-analysis of 11 prospective cohort studies. *J Cell Mol Med*. 2018;22:185–194. doi: 10.1111/jcmm.13307

71. Hai X, Landeras V, Dobre MA, DeOreo P, Meyer TW, Hostetter TH. Mechanism of prominent trimethylamine oxide (TMAO) accumulation in hemodialysis patients. *PLoS One*. 2015;10:e0143731. doi: 10.1371/journal.pone.0143731

72. Osbourn AE, Field B. Operons. *Cell Mol Life Sci*. 2009;66:3755–3775. doi: 10.1007/s00018-009-0114-3

73. Craciun S, Balskus EP. Microbial conversion of choline to trimethylamine requires a glycyl radical enzyme. *Proc Natl Acad Sci U S A.* 2012;109:21307–21312. doi: 10.1073/pnas.1215689109

74. Chen S, Henderson A, Petriello MC, Romano KA, Gearing M, Miao J, Schell M, Sandoval-Espinola WJ, Tao J, Sha B, et al. Trimethylamine N-oxide binds and activates PERK to promote metabolic dysfunction. *Cell Metab.* 2019;30:1141–1151.e5. doi: 10.1016/j.cmet.2019.08.021

75. Seldin MM, Meng Y, Qi H, Zhu W, Wang Z, Hazen SL, Lusis AJ, Shih DM. Trimethylamine N-oxide promotes vascular inflammation through signaling of mitogen-activated protein kinase and nuclear factor-kappaB. *J Am Heart Assoc.* 2016;5:e002767. doi: 10.1161/JAHA.115.002767

76. Moore JO, Hendrickson WA. Structural analysis of sensor domains from the TMAO-responsive histidine kinase receptor TorS. *Structure.* 2009;17:1195–1204. doi: 10.1016/j.str.2009.07.015

77. Devlin AS, Marcobal A, Dodd D, Nayfach S, Plummer N, Meyer T, Pollard KS, Sonnenburg JL, Fischbach MA. Modulation of a circulating uremic solute via rational genetic manipulation of the gut microbiota. *Cell Host Microbe.* 2016;20:709–715. doi: 10.1016/j.chom.2016.10.021